Correlation Equation for Predicting Filter Coefficient Under Unfavorable Deposition Conditions

You-Im Chang and Hsun-Chih Chan
Dept. of Chemical Engineering, Tunghai University, 40704 Taichung, Taiwan

DOI 10.1002/aic.11466
Published online March 13, 2008 in Wiley InterScience (www.interscience.wiley.com).

A new correlation equation for predicting the filter coefficient under unfavorable deposition conditions is presented. By adopting the triangular network model of using the Brownian dynamic simulation method, as the sum of four individual deposition mechanisms, e.g., the Brownian diffusion, the DLVO interactions, the gravitational force, and the interception, the correlation equation is obtained by regressing against a broad range of parameter values governing particle deposition in deep bed filtration. The new correlation equation is able to describe previous experimental results well, especially for those submicro particles with significant Brownian motion behavior. © 2008 American Institute of Chemical Engineers *AIChE J,* 54: 1235–1253, 2008

Keywords: filtration, particle, deposition, correlation, unfavorable condition

Introduction

To find a general correlation equation to predict colloidal deposition rates in granular media of deep bed filters, especially under the unfavorable deposition conditions when the repulsive energy barrier of DLVO theory[1] is presented, is the main goal for many scholars interested in this research area in last two decades. A good review of those studies can be found in the book of Prof. Chi Tien[2] (see Chapter 7). Generally speaking, those correlation equations could not explain the experimental results satisfactorily under the unfavorable deposition conditions. Discrepancies between theoretical predictions and experimental results were always existed when the repulsive energy barrier between colloidal particles and collectors is presented. This problem was not solved until an empirical equation was established by Bai and Tien,[3] which was found to be able to describe those experimental results reasonably well and appears to be much better than any other earlier correlations. By adopting the concept of Vaidyanathan and Tien,[4] they found that those available colloidal filtration data under the unfavorable deposition conditions at various ionic strengths of suspension can be well described by using a filter coefficient α which is defined as the ratio of the initial collection efficiency η_0 to its value in the absence of the electrostatic repulsive force of DLVO theory η_{0S} (i.e., when the ionic strength of the colloidal suspension is high) as

$$\alpha = \frac{\eta_0}{\eta_{0S}} \tag{1}$$

and this filter coefficient α was found to be the function of those parameters used to describe the magnitudes of van der Waals attractive and electrostatic repulsive energies of DLVO theory. Note that this filter coefficient α represents the fractional reduction in the deposition rates of colloidal particles caused by the presence of the repulsive energy barrier of DLVO theory.

In our previous article,[5] by using the Brownian dynamic simulation method and the constricted tube model to rep-

Correspondence concerning this article should be addressed to Y.I. Chang at yichang@thu.edu.tw.

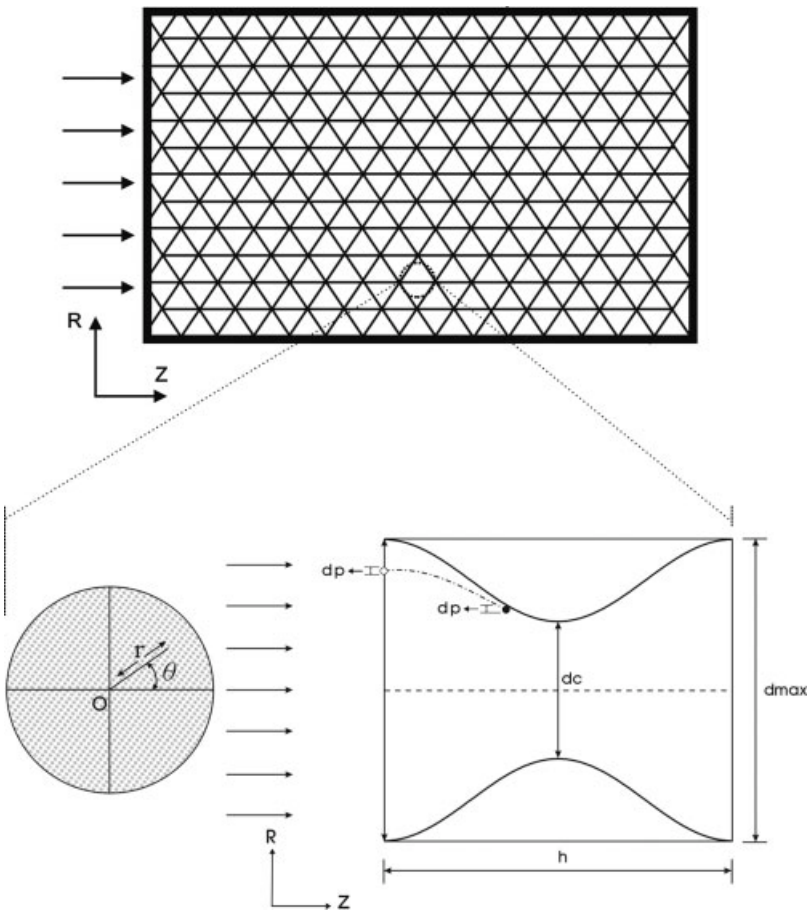

Figure 1. The schematic diagram of the triangular network and the sinusoidal constricted tube model (SCT) adopted in the present article.

The dimensions of the SCT are: $d_{max} = 16.8\ \mu m$, $d_c = 7.2\ \mu m$, and $h = d_g = 20.0\ \mu m$.

resent the pore geometry,[6] we had successfully applied different two-dimensional network models to track the individual particles to move through the porous media of a filter bed (i.e., the Langevin type approach). From which, caused either by the straining or by the direct deposition of particles onto the pore walls, the temporal variations of the effluent concentrations and the pressure drop caused by those deposited particles in the filter were successfully determined. More importantly, when comparing with the available experimental data of measuring filter coefficient, we found that our network model of using the Brownian dynamic simulation method can give smaller discrepancy than that of the convective diffusion model,[7,8] especially under the unfavorable deposition conditions.

By adopting the same definition of filter coefficient given by Eq. 1 and the triangular network model of using the Brownian dynamic simulation method, a more rigorously correlation equation to determine α under unfavorable deposition conditions will be derived in the present paper. This new correlation equation, in addition to those parameters of DLVO theory, the factor of the gravitational force will be also considered.

Network Model

Since the triangular network model of using SCT (sinusoidal constricted tube) gives the best accuracy on predicting the dynamic behavior of granular filtration when comparing with the available experimental data in our previous article,[5] hence here we use the triangular network to represent the porous media of the filter, and adopt the Brownian dynamic simulation method to track the individual particles as they move through the network.[9] All pores in the network and particles in the influent are assumed to be of the Raleigh type size distribution.[10] Then, the pore size distribution can be assigned randomly to the bonds in the network as follows,

$$\int_0^{r'_1} 2r' \exp(-r'^2) dr' = 1 - \exp(-r'^2_1) \tag{2}$$

with

$$r'_1 = \frac{r_f}{r_{mean}} = \sqrt{-\ln(1 - a_i)} \tag{3}$$

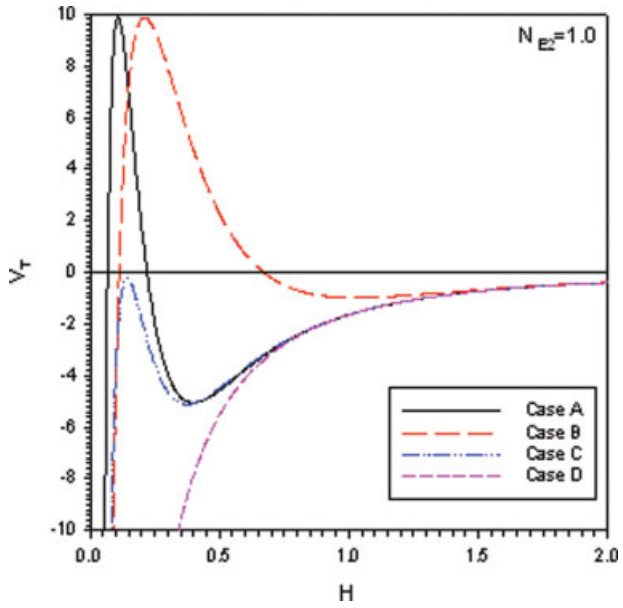

Figure 2. Four different types of the total interaction energy curves of DLVO theory adopted in the simulations of the present article, at which N_{E1} = 105.0 and N_{DL} = 10.75 for curve A, N_{E1} = 50.0 and N_{DL} = 5.02 for curve B, N_{E1} = 77.0 and N_{DL} = 10.0 for curve C, N_{E1} = 0.0 and N_{DL} = 0.0 for curve D, and N_{E2} = 1.0 and N_{Lo} = 7.0 for all four curves.

[Color figure can be viewed in the online issue, which is available at www.interscience.wiley.com.]

and $0 < a_i < 1$ where the random number a_i can be generated by using the standard computer software of IMSL,[11] r_f and r_{mean} are the radius of filter grains and the mean radius of pores, respectively. And the size distribution of the ith particle in the influent is governed by

$$a_{pi} = a_{p,mean}\sqrt{-\ln(1-a_i)} \tag{4}$$

where $a_{p,mean}$ is the mean radius of particles.

In the current model, two different mechanisms of particle capture are considered: straining (size exclusion) and direct deposition. Straining occurs when the particle diameter is larger than the pore diameter selected for it to transport through the network. Straining plugs up the pore, and thereby diverting the flow direction to other available pores. Direct deposition of a particle on a pore wall occurs as a result of hydrodynamic and DLVO interaction forces acting on the particle.[7] The details of this direct deposition mechanism in a constricted tube cell can be found in Chang et al.[12]

Constricted Tube Model

We represent the pore geometry in the present network by the constricted tube model.[6] As shown in Figure 1, the sinusoidal geometric structure (SCT as sinusoidal constricted tube) adopted by Payatakes et al.[6] and Fedkiw and Newman[13] is considered for the constricted tube model in the present study. The expressions of the wall radius r_w corresponding to this SCT geometric structures is:

$$r_w = \frac{r_c + r_{max}}{2}\left[1 + \left(\frac{r_{max} - r_c}{r_{max} + r_c}\right)\cos\left(2\pi\frac{z}{h}\right)\right] \quad \text{for} \quad 0 < \frac{z}{h} < 1 \tag{5}$$

where h is the length of a constricted tube, and its magnitude is equal to the diameter of the grain collector d_g.

For this SCT model, the flow field equations established by Chow and Soda[14] and modified by Chiang and Tien[15] are adopted. The details of these flow field equations can be found in the book of Prof. Tien[2] (see Chapter 3).

Table 1. Summary of Dimensionless Parameters Presented in the Correlation Equation

Parameter	Definition	Physical Interpretation
A_s	$\frac{2(1-\gamma^5)}{2-3\gamma+3\gamma^5-2\gamma^6}$	Porosity-dependent parameter
N_A	$\frac{A}{12\pi\mu a_{pi}^2 U}$	Attraction number
N_{DL}	κa_{pi}	Electric double-layer force parameter
N_{E1}	$va_{pi}(\xi_p^2 + \xi_g^2)/4k_BT$	First electrokinetic parameter
N_{E2}	$2\left(\frac{\xi_p}{\xi_g}\right)\Big/\left[1+\left(\frac{\xi_p}{\xi_g}\right)^2\right]$	Second electrokinetic parameter
N_D	$\frac{2}{9}\frac{a_{Pi}^2(\rho_{Pi}-\rho_f)g}{k_BT}$	Gravity number; ratio of the Stokes particle setting velocity to the approach velocity of the fluid
N_{Pe}	$\frac{Ud_g}{D_\infty}$	Peclet number characterizing ratio of the convective transport to the diffusive transport
N_R	$\frac{d_p}{d_g}$	Aspect ratio
N_{Lo}	$\frac{A}{6k_BT}$	London force parameter

The parameters in the various dimensionless groups are as follows: d_g is the collector diameter, d_p is the particle diameter, U is the inlet fluid velocity, D_∞ is the bulk diffusion coefficient(describe by Stokes-Einstein equation), A is the Hamaker constant, k_B is the Boltzmann constant, T is the fluid absolute temperature, a_{pi} is the ith particle radius, ρ_{pi} is the ith particle density, ρ_f is the fluid density, g is the gravitational acceleration, κ is the reciprocal of the electric double layer thickness, v is the dielectric constant of the fluid, ξ_p and ξ_g are the surface (zeta) potentials of particle and collector, respectively, and $\gamma = (1-\varepsilon)^{1/3}$.

Table 2. Summary of Parameter Values Adopted in the Present Simulations

Parameter	Range
Particle radius, a_{pi}	0.01 ~ 1.0 μm
Collector (grain) diameter, d_g	20 μm
Inlet fluid velocity, U	0.05 ~ 3.0 cm/s
Inlet particle concentration, C_{in}	1000 particles/cm^3
Hamaker constant, A	1.0×10^{-20} J
Fluid absolute temperature, T	293.2 K
Porosity, ε	0.4
Absolute fluid viscosity, μ	1.0 cp
Particle density, ρ_{pi}	1.00 ~ 1.10 g/cm^3

Brownian Dynamics Simulation

Similar to the previous articles by Ramarao et al.[16] and by authors,[12,17] applying the principle of trajectory analysis, the method of Brownian dynamics simulation is adopted in the present study. With consideration of the inertia term in the force balance equation and of the specification of the flow fluid around the collector, the ith particle position in the tube model can be expressed by the Langevin type equation as[2]:in the normal direction

$$r_r = r_r(0) + \left[\left(\frac{f_r^m}{f_r^t}\right)u_r - v_{pr}(0) + \left(\frac{\Delta\rho_i}{\rho_{pi}}\right)\frac{g\sin\alpha'}{\beta C_s f_r^t} - \left(\frac{A_{DLVO}}{f_r^t}\right)\right]\left(\frac{e^{-\beta C_s f_r^t t} - 1}{\beta C_s f_r^t}\right) + \left[\left(\frac{f_r^m}{f_r^t}\right)u_r - \left(\frac{\Delta\rho_i}{\rho_{pi}}\right)\frac{g\sin\alpha'}{\beta C_s f_r^t} - \left(\frac{A_{DLVO}}{f_r^t}\right)\right] t + \frac{1}{\beta C_s f_r^t} \times \int_0^t [1 - e^{-\beta C_s f_r^t (t-r)}]A(\tau)d\tau \qquad (6)$$

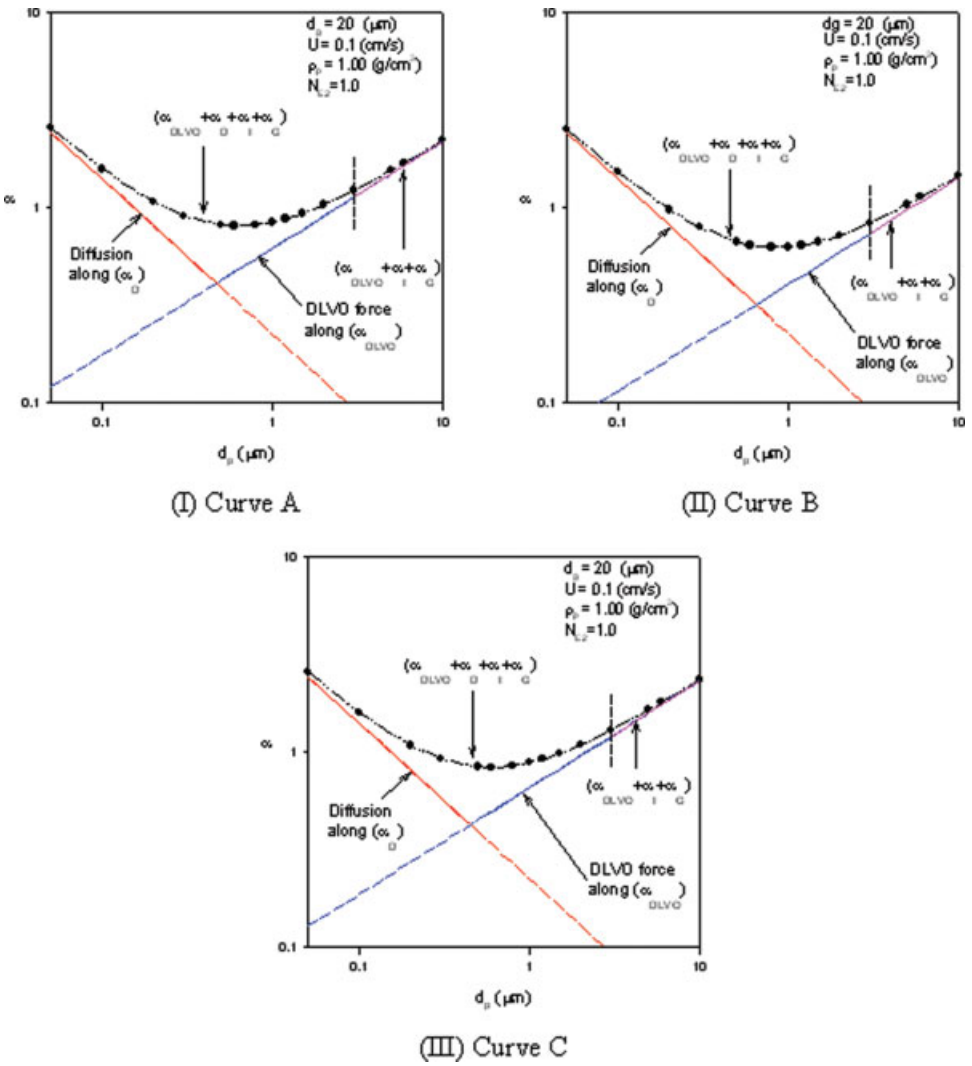

Figure 3. Comparison of predictions of filter coefficients (α) based on solving the trajectory equations (Eqs. 6 and (7) of using the triangular network model (black circles) and the new correlation equation of Eq. 16 (solid lines) corresponding to those different interaction energy curves shown in Figure 2.

In this figure, $\rho_g = 1.00$ g/cm^3, $d_g = 20$ μm, and $U = 0.1$ cm/s. [Color figure can be viewed in the online issue, which is available at www.interscience.wiley.com.]

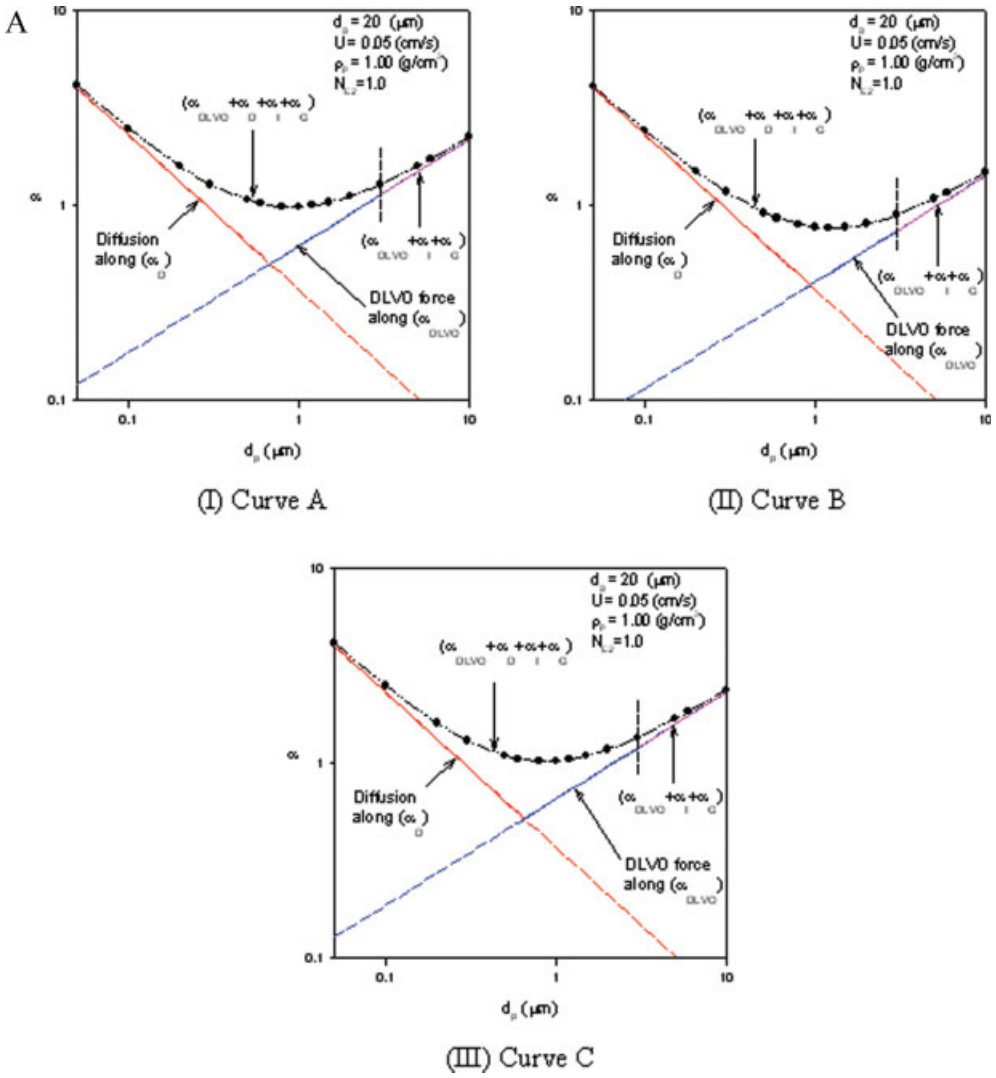

Figure 4. Effect of influent flow rate on the predictions of filter coefficients (α) obtained by using the present Brownian dynamics simulation method corresponding to those different interaction energy curves shown in Figure 2.

With $\rho_g = 1.00\ g/cm^3$ and $d_g = 20\ \mu m$, Figure 4a represents the simulation results when $U = 0.05$ cm/s Figure 4b represents the simulation results when $U = 0.2$ cm/s and Figure 4c represents the simulation results when $U = 0.3$ cm/s. [Color figure can be viewed in the online issue, which is available at www.interscience.wiley.com.]

in the tangential direction

$$r_\theta = r_\theta(0) + \frac{F_3}{C_s\beta}\left[\left(\frac{B\varsigma_2F_1 + C\varsigma_2^2F_2}{B\varsigma_2 + B\varsigma_2^2}\right)u_\theta - v_{p\theta}(0) + \left(\frac{\Delta\rho_i}{\rho_{pi}}\right)g\cos\alpha'\right]\left[e^{-(\beta C_s/F_3)t} - 1\right] + \left[\left(\frac{B\varsigma_2F_1 + C\varsigma_2^2F_2}{B\varsigma_2 + C\varsigma_2^2}\right)u_\theta + \left(\frac{\Delta\rho_i}{\rho_{pi}}\right)g\cos\alpha'\left(\frac{F_3}{C_s\beta}\right)\right]t + \frac{F_3}{C_s\beta}\int_0^t [1 - e^{-(\beta C_s/F_3)(t-\tau)}]A(\tau)d\tau \quad (7)$$

with $A_{DLVO} = \frac{1}{m_{pi}\beta C_s}(F_{Lo} + F_{DL})$, and $\beta = \frac{6\pi\mu a_{pi}}{C_s m_{pi}}$ where $v_{pr}(0)$ and $v_{p\theta}(0)$ are the initial velocities of particles in the normal and tangential directions, respectively, m_{pi} is the mass of the ith particle, a_{pi} is the radius of the ith particle, ρ_{pi} is the density of the ith particle, $\Delta\rho_i$ is the density difference between the fluid and the ith particle, μ is the viscosity of the fluid, C_s is the Cunningham correction factor which is equal to 1.16 for hydrosols, β is the friction coefficient per unit mass of the particle, t is the time, F_{Lo} and F_{DL} are the van der Waals attractive force and the electric double layer repulsive force of DLVO theory, respectively, and their definitions of $F_{Lo} = \nabla\phi_{Lo}$ and $F_{DL} = \nabla\phi_{DL}$ will be given later. Also, those factors of F_1, F_2, F_3, f_r^m, and f_r^t shown in Eqs. 6 and 7 are the hydrodynamic retardation factors of normal vector, drag force, and shear vector, and their numerical values at different separation distances can be found in Tables 5.1 and 5.3 of ref. 2, and $A(t)$ represents a Gaussian white noise process in stochastic terms.[18] In Eq. 7, ς_2 is the normal coor-

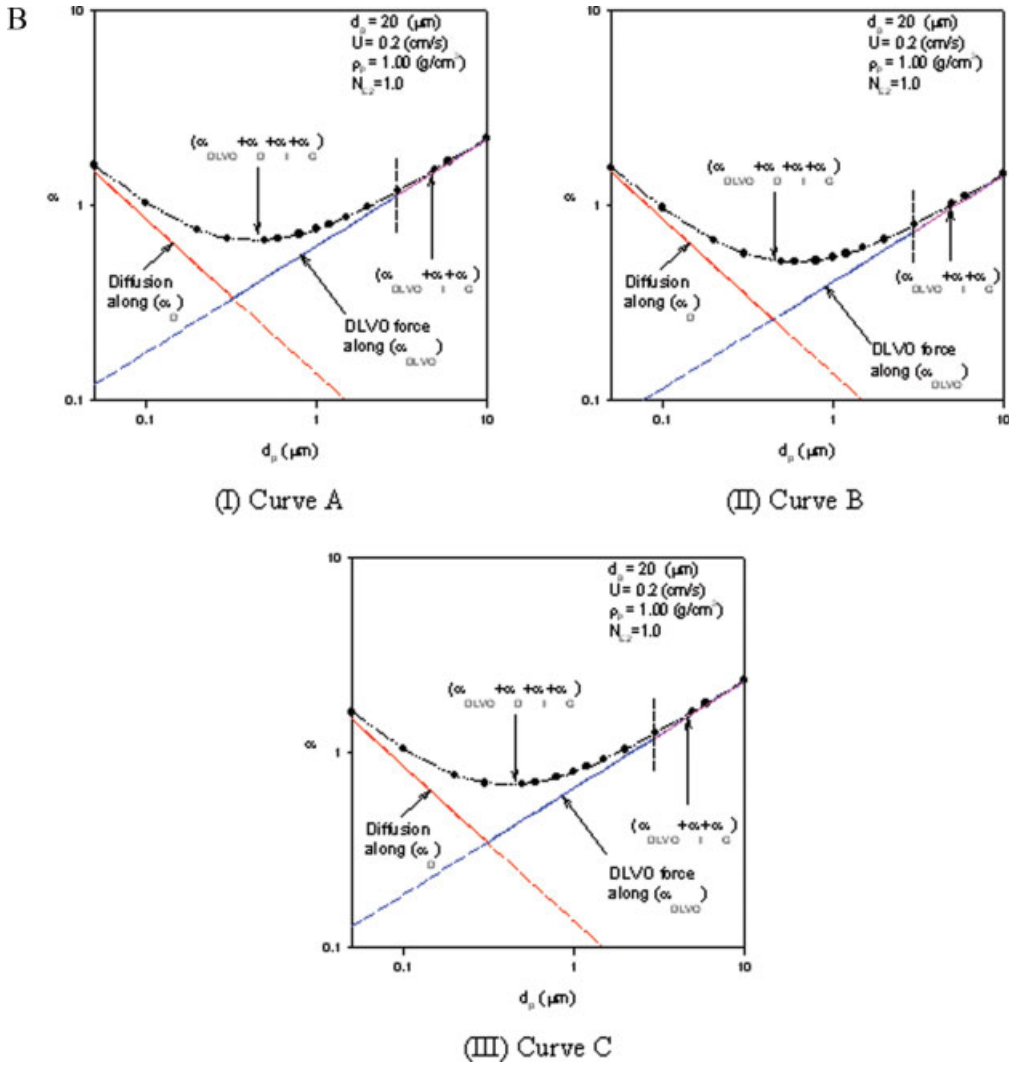

Figure 4. Continued

dinate of the particle center, and B and C are the polynomial coefficients to represent the tangential component of the undisturbed flow field u_θ in the proximity of the collector surface,

$$u_\theta = B\varsigma_2 + C\varsigma_2^2 \tag{8}$$

where the values of B and C are dependent on the geometry of the collector, and their evaluation method can be found in chapter 5.8 of ref. 2. From those trajectories of influent particles in the network, the temporal variations of the effluent concentrations and the pressure drop in a filtration history can be obtained,[9] and therefore the values of the initial collection efficiency η_0 and the filter coefficient α shown in Eq. 1 can be determined consequently.

The Interaction Energy Curve of DLVO Theory

In the present article, to take account of those parameters describing the magnitudes of energy barriers of DLVO theory, the effects of four different types of total interaction energy curves (see Figure 2) on determining α will be investigated by using the triangular network model of using SCT mentioned above.

According to the DLVO theory,[1] the total interaction energy barrier between two approaching colloidal particles is the algebraic sum of the van der Waals and the electrostatic double layer potentials as follows (see Chapter 5.4 of Ref. 2):

$$\frac{V_T}{k_B T} = \phi_{Lo} + \phi_{DL} \tag{9}$$

with

$$\phi_{Lo} = -N_{Lo}\left[\frac{2(H+1)}{H(H+2)} + \ln H - \ln(H+2)\right]$$

(with the unit of $k_B T$)

$$\phi_{DL} = N_{E1}\left\{N_{E2}\ln\left[\frac{1+\exp(-X)}{1-\exp(-X)}\right] + \ln[1-\exp(-2X)]\right\}$$

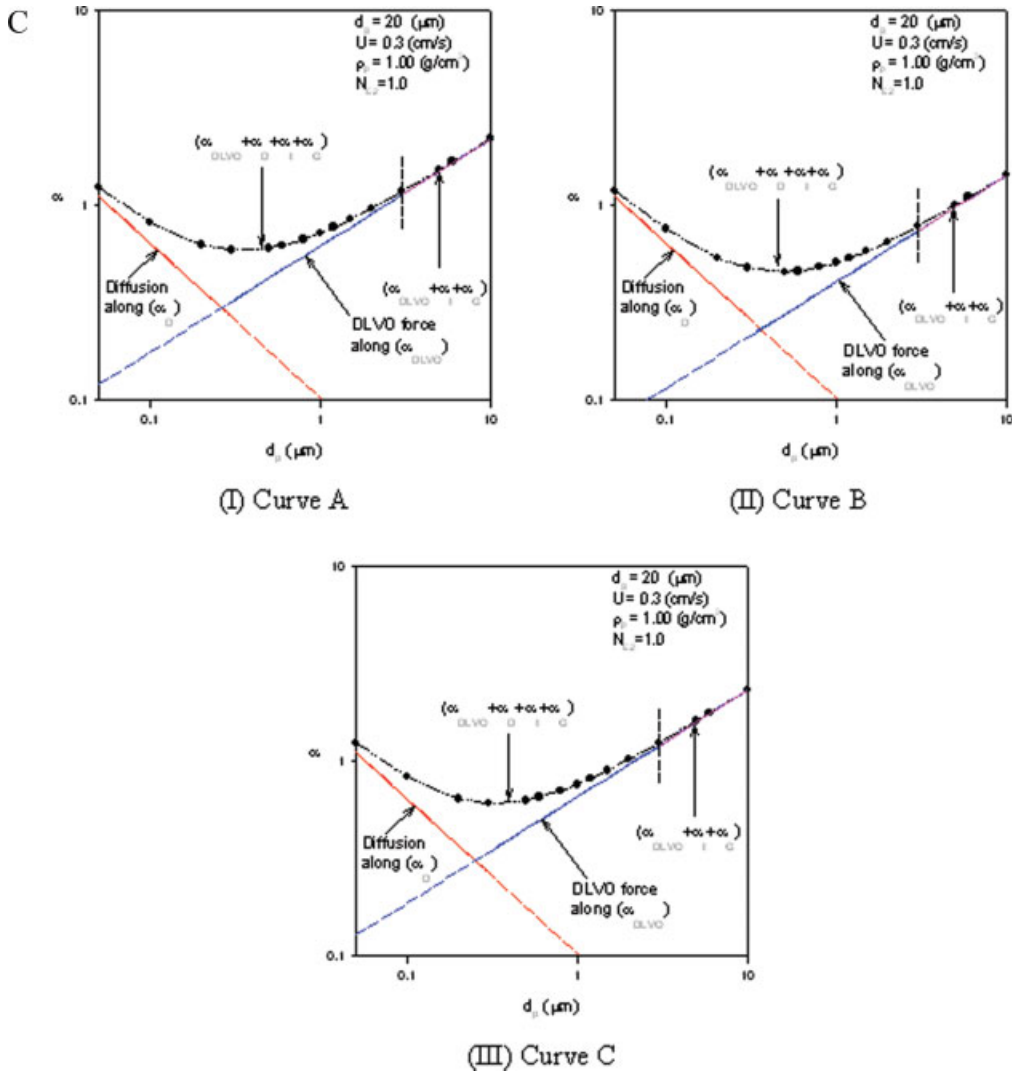

Figure 4. Continued

(with the unit of k_BT), where

$$H = \frac{h_s}{a_{pi}}, \quad N_{Lo} = \frac{A}{6k_BT}, \quad N_{DL} = \kappa a_{pi}, \quad X = N_{DL}H,$$

$$N_{E1} = v\frac{a_{pi}(\xi_p^2 + \xi_g^2)}{4k_BT}, \quad N_{E2} = 2\left(\frac{\xi_p}{\xi_g}\right)\Big/\left[1 + \left(\frac{\xi_p}{\xi_g}\right)^2\right].$$

The definitions of those parameters shown in the above equations will be given in the notation section later.

As shown in Figure 2, curves A exhibits a large primary maximum energy barrier $V_{p,max}$ and a deep secondary energy minimum $V_{s,min}$, curve B a large primary maximum energy barrier and a negligible secondary energy minimum, curve C a deep secondary energy minimum only and curve D a ''barrierless'' interaction energy curve, respectively. In this figure, $N_{E1} = 105.0$ and $N_{DL} = 10.75$ for curve A, $N_{E1} = 50.0$ and $N_{DL} = 5.02$ for curve B, $N_{E1} = 77.0$ and $N_{DL} = 10.0$ for curve C, $N_{E1} = 0.0$ and $N_{DL} = 0.0$ for curve D, and $N_{E2} = 1.0$ and $N_{Lo} = 7.0$ for all four curves. The effects of those parameters N_{Lo}, N_{DL}, N_{E1}, and N_{E2} on the deposition rates of Brownian particles were already studied in our previous paper systematically,[17] where the pore structures were represented by the spherical collector and the constructed tube model, respectively. By calculating the collection efficiencies of particles in SCT, we also found that the collection efficiency of curve D is always greater than those of curves A, B and C when Reynolds number of fluid is small because there is no energy barrier exists, and the deposition mechanism of particles is controlled by the Brownian diffusion effect. For curve A, it was found that, even with the presence of the deep secondary minimum which increases the accumulation probability of the particles, the steepest slope between the secondary minimum and the primary maximum energy barriers of curve A is still the main reason for its low collection efficiency. The existence of the primary maximum energy barrier in the total interaction energy curves of A and B was found unfavorable for those colloidal particles to deposit on the pore walls in the filter.[12,17] As pointed out by

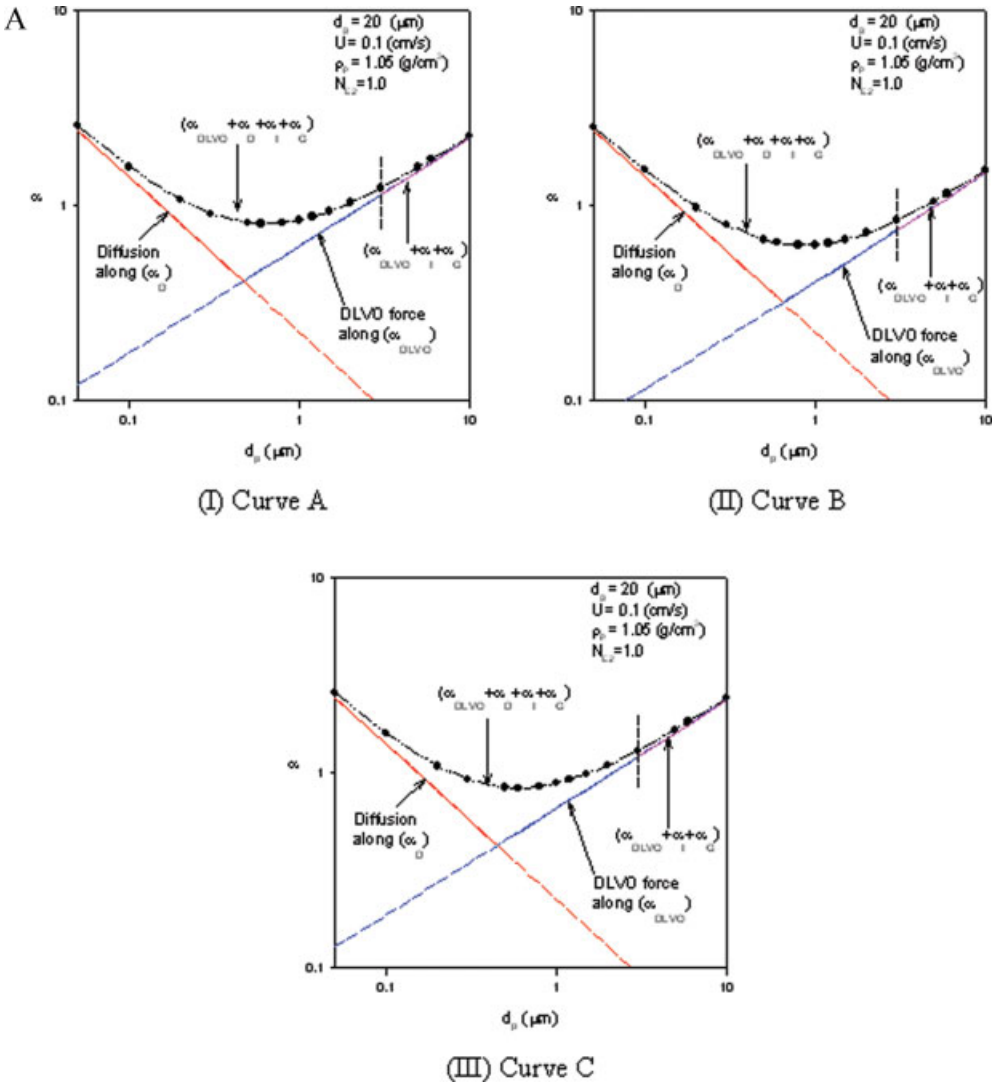

Figure 5. Effect of the gravitational force on the predictions of filter coefficients (α) obtained by using the present Brownian dynamics simulation method corresponding to those different interaction energy curves shown in Figure 2.

With $d_g = 20$ μm and $U = 0.1$ cm/s, Figure 5a represents the simulation results when $\rho_g = 1.05$ g/cm^3, and Figure 5b represents the simulation results when $\rho_g = 1.10$ g/cm^3. [Color figure can be viewed in the online issue, which is available at www.interscience.wiley.com.]

Rajagopalan and Kim[19] that the deposition rate of particles (i.e., in terms of the Sherwood number) is proportional to $\exp(-0.96\ V_{p,max})$ when $V_{p,max} \geq 5.0\ k_BT$ and $V_{s,min} \leq 0.5\ k_BT$. Therefore, when comparing with that of ''barrierless'' interaction energy curve D, the value of $V_{p,max} = 10.0\ k_BT$ in curve A will reduce its corresponding deposition rate of particles by about five orders of magnitude which is big enough to fulfill the unfavorable deposition condition described in the present study. Corresponding to the triangular network model of using SCT shown in Figure 1 and those four types of interaction energy curves shown in Figure 2, the simulation works of determining the filter coefficient α at various values of particle sizes under different influent flow rates and gravitational forces will be conducted first in the present study. By applying those simulation results with the method of nonlinear regression, a new correlation equation for determining α will be derived as follows.

Correlation Equation

Accurate predictions of the dynamic filtration behavior of colloidal particles can be obtained either by solving the convective diffusion equation[7,8] or by using the method of trajectory analysis.[6] Results of such rigorously approach reveal that the aspect ratio, the influent flow rate, the gravitational force, and the parameters determine the magnitudes of energy barriers of DLVO theory, all play important roles in describing the filtration behavior of colloidal particles. When written in the dimensionless groups forms, the initial collection efficiency η_0 can be expressed as a function of

$$\eta_0 = \eta_0(N_R, N_{Pe}, N_G, N_A, N_{Lo}, N_{DL}, N_{E1}, N_{E2}) \qquad (10)$$

where N_R is an aspect ratio, N_{Pe} is the Peclet number, N_G is the gravitational number, N_A is the attraction number, N_{Lo} is the van der Waals number, N_{DL} is the electric double layer number (i.e.,

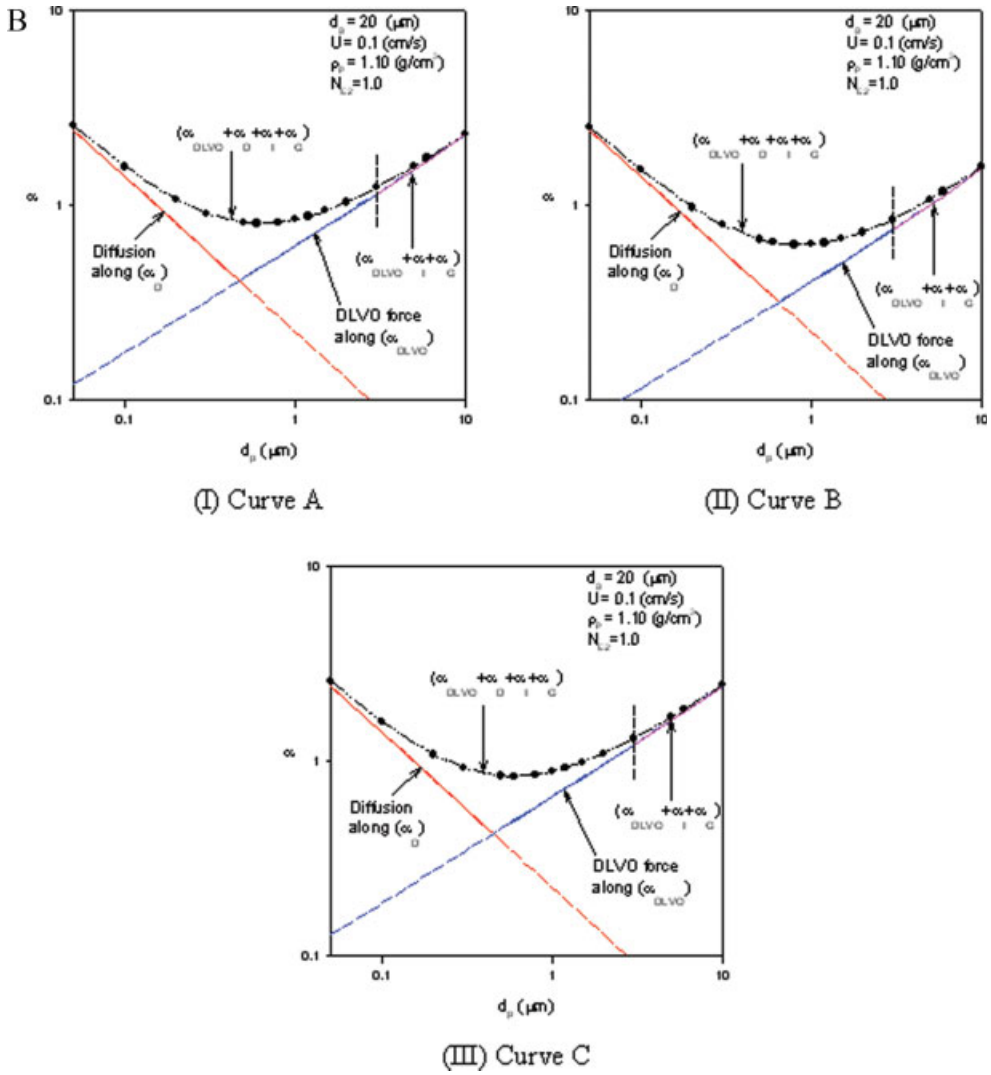

Figure 5. Continued

$N_{DL} \gg 1.0$ means $a_{pi} \gg \kappa^{-1}$), N_{E1} and N_{E2} are the first and the second electrokinetic numbers of the DLVO theory, respectively. The definitions of these dimensionless numbers are provided in Table 1. There are many correlation equations derived in the last two decades, and a good summary can be found in the book of Chi Tien[2] (see Chapter 7). Some of the important correlation equations are briefly introduced as follows.

Assuming the three deposition mechanisms, namely diffusion η_D, interception η_I, and gravitational force η_G are additive, Yao's model[20] is the first water filtration model can successfully predict the initial collection efficiency η_0 by numerically solving a simplified convective diffusion around a spherical collector for the various sizes of colloidal particles.

$$\eta_0 = \eta_D + \eta_I + \eta_G \tag{11}$$

with $\eta_D = 4.04\, A_S^{1/3} N_{Pe}^{-2/3}$

$$\eta_I = \frac{3}{2} A_S N_R^2$$

$$\eta_G = \frac{(\rho_p - \rho)}{18\mu U} g d_p^2.$$

Here, by using Happel's sphere-in-cell model,[21] A_S is the porosity dependent parameter defined as

$$A_S = \frac{2(1-\gamma^5)}{2-3\gamma+3\gamma^5-2\gamma^6} \tag{12}$$

where $\gamma = (1-\varepsilon)^{1/3}$, and ε is the porosity of the filter. However, the effects of the hydrodynamic interactions and the interaction energy barriers of DLVO theory were not considered in this classic filtration equation.

A more rigorous approach that includes hydrodynamic retardation corrections for the favorable surface interactions was developed by Rajagopalan and Tien.[22] Based on numerical solutions of the trajectory analyses made with a sphere-in-cell porous media model under various physical conditions, a correlation equation was obtained as

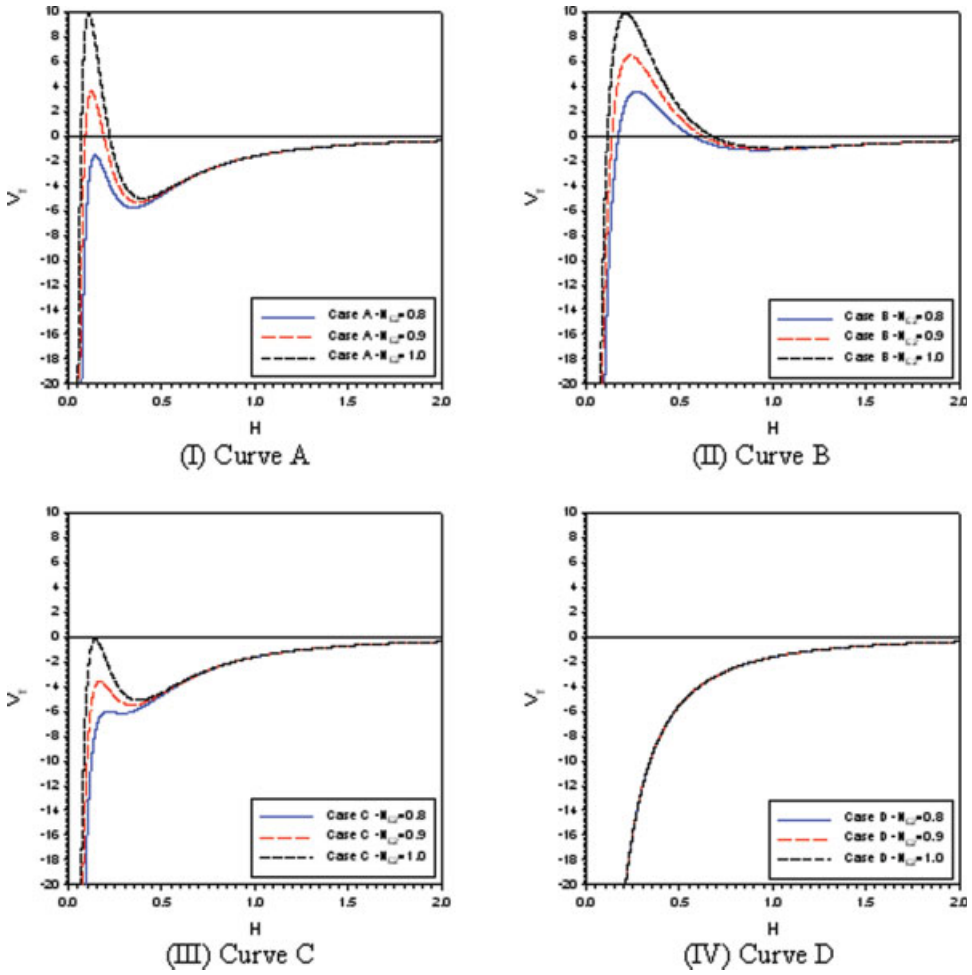

Figure 6. Effect of changing N_{E2} value on the profiles of those four different interaction energy curves shown in Figure 2.

[Color figure can be viewed in the online issue, which is available at www.interscience.wiley.com.]

$$\eta_0 = (1-\varepsilon)^{2/3} A_s N_{Lo}^{1/8} N_R^{15/8} + (3.375 \times 10^{-3})(1-\varepsilon)^{2/3} A_S N_G^{1.2} N_R^{-0.4} + 4(1-\varepsilon)^{2/3} A_S^{1/3} N_{Pe}^{-2/3}. \quad (13)$$

This equation was found to be accurate enough in the interception range as well as the diffusion dominated region. Later on, by solving the convective diffusion equation with a perfect sink boundary condition, Tufenkij and Elimelech[23] obtained a modified correlation equation for describing the initial collection efficiency of colloidal particles onto a single spherical collector as

$$\eta_0 = \eta_D + \eta_I + \eta_G = 2.4 A_S^{1/3} N_R^{-0.081} N_{Pe}^{-0.715} N_{Lo}^{0.052} + 0.55 A_S N_R^{1.675} N_A^{0.125} + 0.22 N_R^{-0.24} N_G^{1.11} N_{Lo}^{0.053} \quad (14)$$

This modified correlation equation showed remarkable agreement with those experimental results where electrostatic double layer interactions were negligible.

Unfortunately, all the above correlation equations were inadequate for the unfavorable deposition conditions where the electrostatic repulsion force may prevent particles from reaching the filter grain surfaces. This problem was not solved until Bai and Tien[3] who adopted the concept suggested by Vaidyanathan and Tien[4] earlier that the deposition rates of colloidal particles under unfavorable surface interactions at various ionic strengths can be well correlated by using the filter coefficient α as defined in Eq. 1. After comparing with many available experimental data by using the regression technique, they found a subtle correlation equation of α as

$$\alpha = \frac{\eta_0}{\eta_{0S}} = 2.527 \times 10^{-3} N_{Lo}^{0.7031} N_{E1}^{-0.3121} N_{E2}^{3.5111} N_{DL}^{1.352} \quad (15)$$

with $N_{Lo} = \dfrac{4A}{9\pi\mu d_p^2 U}$, $N_{E1} = \dfrac{v(\xi_p^2 + \xi_g^2)}{3\pi\mu d_p U}$, $N_{E2} = \dfrac{2\xi_p \xi_g}{(\xi_p^2 + \xi_g^2)}$

and $N_{DL} = \kappa d_p$.

In Eq. 15, the factor of the gravitational force was not included in this correlation equation. To amend this deficiency, the derivation of a new correlation equation of α by adopting the triangular network model of using the Brownian

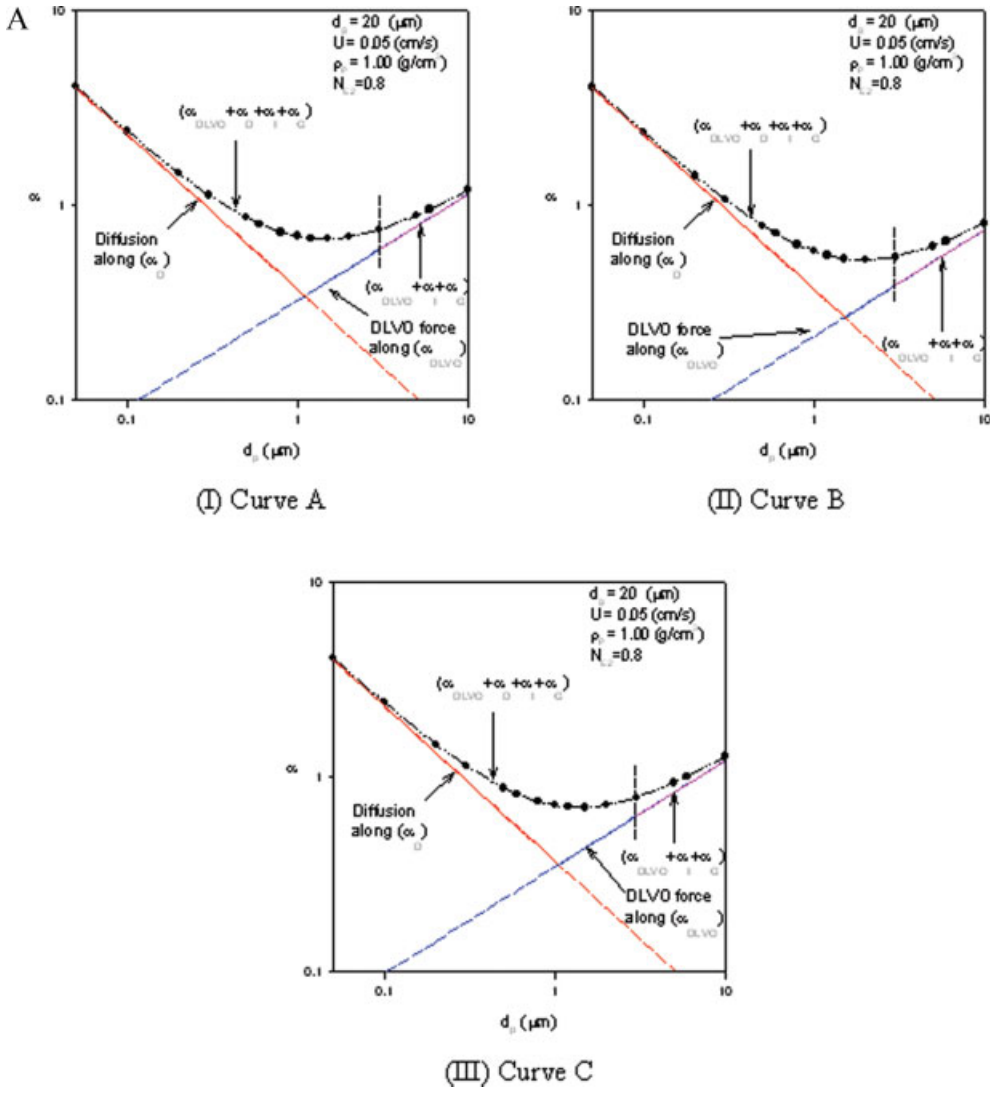

Figure 7. Effect of changing N_{E2} value on the predictions of filter coefficients (α) obtained by using the present Brownian dynamics simulation method corresponding to those different interaction energy curves shown in Figure 6.

With $\rho_g = 1.00$ g/cm^3, $d_g = 20$ μm, and $U = 0.05$ cm/s, Figure 7a represents the simulation results when $N_{E2} = 0.8$ and Figure 7b represents the simulation results when $N_{E2} = 0.9$. [Color figure can be viewed in the online issue, which is available at www.interscience.wiley.com.]

dynamic simulation method will be given below. In this new correlation equation, all of those dimensionless groups shown in Eq. 10 will be included.

Simulation Results and Discussion

Simulations are performed first on a triangular two-dimensional network with $N_L = 210 \times 72$ to obtain a new correlation equation. The parameter values adopted in the present simulations are given in Table 2. In the present simulations, corresponding to those different values of particle size, influent flow rate, and the gravitation force shown in Table 2, the simulation results on determining those initial collection efficiencies obtained from the ''barrierless'' interaction energy curve D will be regarded as the value of η_{0S}, while those obtained values from curves A, B, and C illustrated in Figure 2 will be adopted as the value of η_0 shown in Eq. 1. Then, by comparing with those available experimental results provided by Bai and Tien,[3] Elimelech and O'Melia,[24] Elimelech,[25] and Vaidyanathan and Tien,[26] the accuracy of the present correlation equation will be studied in a later section.

The effects of interaction energy curves of DLVO theory

Figure 3 shows the predicted filter coefficient as a function of the particle size corresponding to those different interaction energy curves shown in Figure 2. For smaller particles (i.e., when $d_P < 0.5$ μm), because of the decreased Brownian

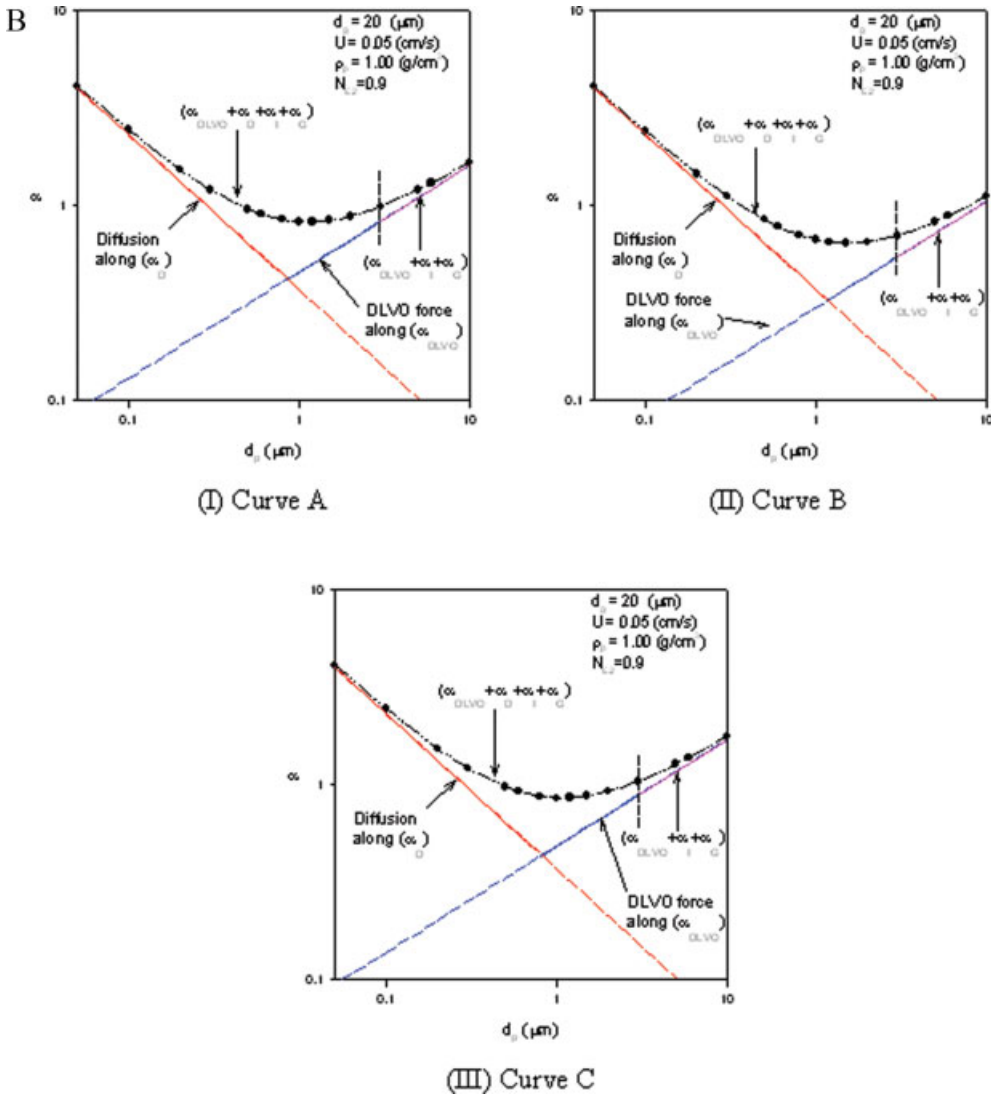

Figure 7. Continued

diffusion effect as particle size increases, the filter coefficient will decrease. After passing through the minimum (i.e., α_{min} at $d_P = 0.5$ μm), the filter coefficient will rise rapidly as particle size increases. In our simulations, we found that those DLVO interaction forces of Eq. 7 are the dominate factors on determining the magnitudes of α when 0.5 μm $< d_P <$ 3.0 μm, while the mechanisms of interception and gravitational force become gradually important when $d_P \geq 3.0$ μm (i.e., indicated by the vertical dashed lines as shown in Figures 3a,b).

Effects of influent flow rate and the gravitational force

To demonstrate the versatility of the present correlation equation, more representative simulation results of α vs. d_P under different influent flow rates and the gravitational forces are given in Figures 4 and 5, respectively. When comparing Figures 4a–c with the corresponded figures of Figure 3 for the same interaction energy curve, we can find that the increased flow rate does not affect those α values at the regions of DLVO forces, interception and gravitational mechanisms control (i.e., when $d_P > 0.5$ μm). However, the α values on the left hand side of α_{min} will decrease with the increase of influent flow rate, and this decreasing rate becomes pronounced for smaller particle size where the diffusion mechanism dominates the whole deposition process. The effect of increasing the gravitational force on the filter coefficient is observed in Figures 5a, b. Different with the increasing in flow rate, the increase of the gravitational force can only slightly increase those α values at the region $d_P \geq$ 3.0 μm where the gravitational force and the interception mechanism dominate.

Effect of changing the value of N_{E2}

Since the values of N_{E2} given for those four interaction energy curves shown in Figure 2 are all fixed at $N_{E2} = 1.0$, hence we have also investigated the effect of changing the

Table 3. Summary of Experimental Data Adopted From the Studies of Bai and Tien,[3] Elimelech and O'Melia,[24] Elimelech,[25] and Vaidyanathan and Tien[26]

References	Exp. No.	NaCl (M)	d_P (μm)	d_g (mm)	ξ_P (mV)	ξ_g (mV)	U (cm/s)	T (°C)	α
Vaidyanathan and Tien[4]	1	0.181	11.4	0.345	−1	−3	2.000	20	1.0000
	2	0.181	11.4	0.345	−1	−3	3.000	20	0.7937
	3	0.181	11.4	0.345	−1	−3	4.000	20	0.6343
	4	0.181	6.1	0.345	−1	−3	2.000	20	0.9086
	5	0.096	11.4	0.345	−1	−3	2.000	20	0.6599
	6	0.01	11.4	0.345	−11	−13	2.000	20	0.2892
	7	0.181	11.4	0.345	−1	−3	2.000	20	1.0000
	8	0.181	11.4	0.345	−1	−3	3.000	20	0.5341
	9	0.181	11.4	0.345	−1	−3	4.000	20	0.5341
	10	0.181	6.1	0.345	−1	−3	2.000	20	0.7503
	11	0.096	11.4	0.345	−1	−3	2.000	20	0.4685
	12	0.01	11.4	0.345	−11	−13	2.000	20	0.2130
Elimelech and O'Melia[24]	1	0.3	0.753	0.2	−28.2	−17.5	0.136	25	0.6457
	2	0.1	0.753	0.2	−41.0	−29.3	0.136	25	0.4467
	3	0.03	0.753	0.2	−62.3	−39.0	0.136	25	0.1585
	4	0.01	0.753	0.2	−80.0	−47.5	0.136	25	0.0407
	5	0.003	0.753	0.2	−89.5	−56.4	0.136	25	0.0195
Elimelech[25]	1	0.00316	0.121	0.2	−76	−57	0.136	25	0.0107
	2	0.01	0.121	0.2	−61	−47	0.136	25	0.0324
	3	0.01778	0.121	0.2	−51	−43	0.136	25	0.0724
	4	0.03162	0.121	0.2	−37	−39	0.136	25	0.1585
	5	0.05623	0.121	0.2	−33	−33	0.136	25	0.3020
	6	0.001	0.121	0.2	−86	−61	0.136	25	0.0028
	7	0.00316	0.378	0.2	−96	−57	0.136	25	0.0110
	8	0.01	0.378	0.2	−86	−47	0.136	25	0.0251
	9	0.01778	0.378	0.2	−70	−43	0.136	25	0.0490
	10	0.03162	0.378	0.2	−55	−39	0.136	25	0.0977
	11	0.05623	0.378	0.2	−43	−33	0.136	25	0.2042
	12	0.001	0.753	0.2	−89	−61	0.136	25	0.0089
	13	0.00316	0.753	0.2	−87	−57	0.136	25	0.0155
	14	0.01	0.753	0.2	−81	−47	0.136	25	0.0372
	15	0.01778	0.753	0.2	−71	−43	0.136	25	0.0676
	16	0.03162	0.753	0.2	−62	−39	0.136	25	0.1514
	17	0.05623	0.753	0.2	−50	−33	0.136	25	0.3162
Bai and Tien[3]	1	0	3.004	0.46	−20.5	−25	0.103	23	0.0076
	2	0.0001	3.004	0.46	−19.6	−22.8	0.103	23	0.0098
	3	0.001	3.004	0.46	−18.1	−21.2	0.103	21.5	0.0552
	4	0.01	3.004	0.46	−13.9	−18.1	0.103	22	0.2126
	5	0.1	3.004	0.46	−6	−11.2	0.103	22.5	0.9700
	6	0.2	3.004	0.46	−5.1	−8	0.103	22.5	1.0000
	7	0.1	3.004	0.46	−6	−11.2	0.103	21.8	0.9733
	8	0.0001	0.802	0.46	−20.7	−22.8	0.103	21	0.0039
	9	0.0001	0.802	0.46	−20.7	−22.8	0.169	21	0.0029
	10	0.0001	0.802	0.46	−20.7	−22.8	0.272	21	0.0024
	11	0.001	0.802	0.46	−19.3	−21.2	0.103	23.3	0.0453
	12	0.01	0.802	0.46	−15.7	−18.1	0.103	22.8	0.1704
	13	0.01	0.802	0.46	−15.7	−18.1	0.169	22.8	0.1562
	14	0.01	0.802	0.46	−15.7	−18.1	0.272	22.8	0.1506
	15	0.1	0.802	0.46	−7	−11.2	0.103	21.5	0.7010
	16	0	3.063	0.35	−25.5	−16.4	0.103	22.5	0.0049
	17	0	3.063	0.35	−25.5	−16.4	0.169	22.5	0.0071
	18	0	3.063	0.35	−25.5	−16.4	0.272	22.5	0.0068
	19	0.0001	3.063	0.35	−24.5	−12.9	0.103	24	0.0085
	20	0.0001	3.063	0.35	−24.5	−12.9	0.169	24	0.0088
	21	0.0001	3.063	0.35	−24.5	−12.9	0.272	24	0.0074
	22	0.001	3.063	0.35	−23	−11	0.103	24	0.0226
	23	0.001	3.063	0.35	−23	−11	0.169	23	0.0236
	24	0.001	3.063	0.35	−23	−11	0.272	24	0.0233
	25	0.01	3.063	0.35	−15	−8	0.103	23.5	0.1360
	26	0.01	3.063	0.35	−15	−8	0.169	21	0.1700
	27	0.01	3.063	0.35	−15	−8	0.272	24	0.1749
	28	0.03	3.063	0.35	−10	−5	0.103	21.5	0.3119
	29	0.03	3.063	0.35	−10	−5	0.169	21.5	0.3099
	30	0.03	3.063	0.35	−10	−5	0.272	21.5	0.3304
	31	0.06	3.063	0.35	−8	−4	0.103	22	0.6430
	32	0.06	3.063	0.35	−8	−4	0.169	22	0.6555
	33	0.06	3.063	0.35	−8	−4	0.272	22	0.6888
	34	0.1	3.063	0.35	−6.8	−3	0.103	23.5	0.9569

Table 3. (Continued)

References	Exp. No.	NaCl (M)	d_P (μm)	d_g (mm)	ξ_P (mV)	ξ_g (mV)	U (cm/s)	T (□)	α
	35	0.1	3.063	0.35	−6.8	−3	0.169	23.5	0.9584
	36	0.1	3.063	0.35	−6.8	−3	0.272	22.5	0.9408
	37	0.2	3.063	0.35	−5.5	−2	0.103	23.5	1.0000
	38	0.2	3.063	0.35	−5.5	−2	0.169	24	1.0000
	39	0.2	3.063	0.35	−5.5	−2	0.272	25	1.0000
	40	0	3.063	0.35	−25.5	−16.4	0.103	23	0.0054
	41	0.001	3.063	0.35	−23	−11	0.103	23	0.0253
	42	0.01	3.063	0.35	−15	−8	0.103	23	0.1859
	43	0.1	3.063	0.35	−6.8	−3	0.103	23	0.9431
	44	0.1	3.063	0.35	−6.8	−3	0.103	23	0.9589
	45	0.1	3.063	0.35	−6.8	−3	0.103	22	0.9900

value of N_{E2} on the accuracy of the present correlation equation Eq. 16 obtained below. Figures 6a and b, c and d illustrate the corresponded energy curves for all of those four interaction energy curves when their values of N_{E2} are increased from $N_{E2} = 0.8$ to $N_{E2} = 1.0$. For curves A, B, and C, we find that the heights of the primary maximum energy barriers increase as N_{E2} increases, which will cause smaller collection efficiencies consequently. However, for curve D, its profile is not affected by changing the value of N_{E2}. Corresponding to those energy curves of different N_{E2} values shown in Figure 6, the simulation results on determining α values are shown in Figures 7a, b. When comparing those results of Figures 7a, b with the corresponding energy curves of Figure 2, we can find that the increase of N_{E2} value will only increase those α values on the right hand side of α_{min} where the DLVO forces dominate. This result of increasing α values is caused by the fact that, because the increased height of the primary maximum energy barrier is unfavorable for those particles to deposit at the entrance region of the filter and can transport more particles moving inside the network to increase their probability of deposition or plugging smaller pores (i.e., straining effect), and therefore the corresponded η_0 values of Eq. 1 will increase with the increase of N_{E2} value. Note that the η_{0S} value of Eq. 1 does not change with the increase of N_{E2} value, since its corresponded profile of curve D is not affected at all as shown in Figure 6.

The new correlation equation

Based on those previous correlation equations mentioned earlier and those simulation results obtained as shown in Figures 3–5 and 7, by applying the multiple nonlinear regression program of SPSS,[27] a new correlation equation of predicting the filter coefficient can be obtained as follows,

$$\alpha = \alpha_{DLVO} + \alpha_D + \alpha_I + \alpha_G = 0.024 N_{DL}^{0.969} N_{E1}^{-0.423} N_{E2}^{2.880} N_{Lo}^{1.5} + 3.176 A_S^{1/3} N_R^{-0.081} N_{Pe}^{-0.715} N_{Lo}^{2.687} + 0.222 A_S N_R^{3.041} N_{Pe}^{-0.514} N_{Lo}^{0.125} + N_R^{-0.24} N_G^{1.11} N_{Lo}. \quad (16)$$

In Eq. 16, the dimensionless groups considered for the term of α_{DLVO} are the same as those considered by Bai and Tien,[3] while those groups shown in the terms of α_D, α_I, and α_G are similar with those adopted by Rajagopalan and Tien[22] and Tufenkij and Elimelech[23] who had obtained correlation equations based on the initial collection efficiencies under the favorable deposition conditions only. As shown in Figures 3–5 and 7, it can be found that the four terms of different deposition mechanisms shown in Eq. 16 can well predict those theoretical results on predicting α values obtained by using the present network model of using the Brownian dynamics simulation method.

Comparison of new correlation with experimental data

In the present article, those experimental results provided by Bai and Tien,[3] Elimelech and O'Melia,[24] Elimelech,[25] and Vaidyanathan and Tien[26] will be adopted for testing the accuracy of the present new correlation equation. Their experimental conditions are summarized according to different ionic strengths in Table 3. For those experimental conditions when the ionic strengths of suspensions are smaller than 0.2 M, we found that their corresponded total interaction energy curves are similar to that of the type B curve shown in Figure 2 and therefore belong to the unfavorable deposition conditions. For the experiments of Elimelech and O'Melia[24] and Elimelech,[25] the cases of four different particle sizes at fixed collector diameter and influent flow rate are adopted for comparison. While for those experiments of Bai Tien,[3] in addition to the particle size, the cases of different collector diameters and influent flow rates are also adopted for comparisons. For the experiments of Vaidyanathan and Tien,[26] the cases of three different ionic strengths at a fixed influent flow rate $U = 0.2$ cm/sec when $d_p = 11.4$ μm are adopted for comparison in the present article.

By comparing with the correlation equation established by Bai and Tien,[3] the predictions of the present new correlation equation are demonstrated in Figures 8 and 9, where the filter coefficients corresponding to those experimental conditions of Table 3 are calculated at different ionic strengths by the following equation when the breakthrough moment is achieved,

$$\eta_0 = \frac{2 d_g}{3(1-\varepsilon)L} \ln\left(\frac{C_{in}}{C_{eff}}\right) \quad (17)$$

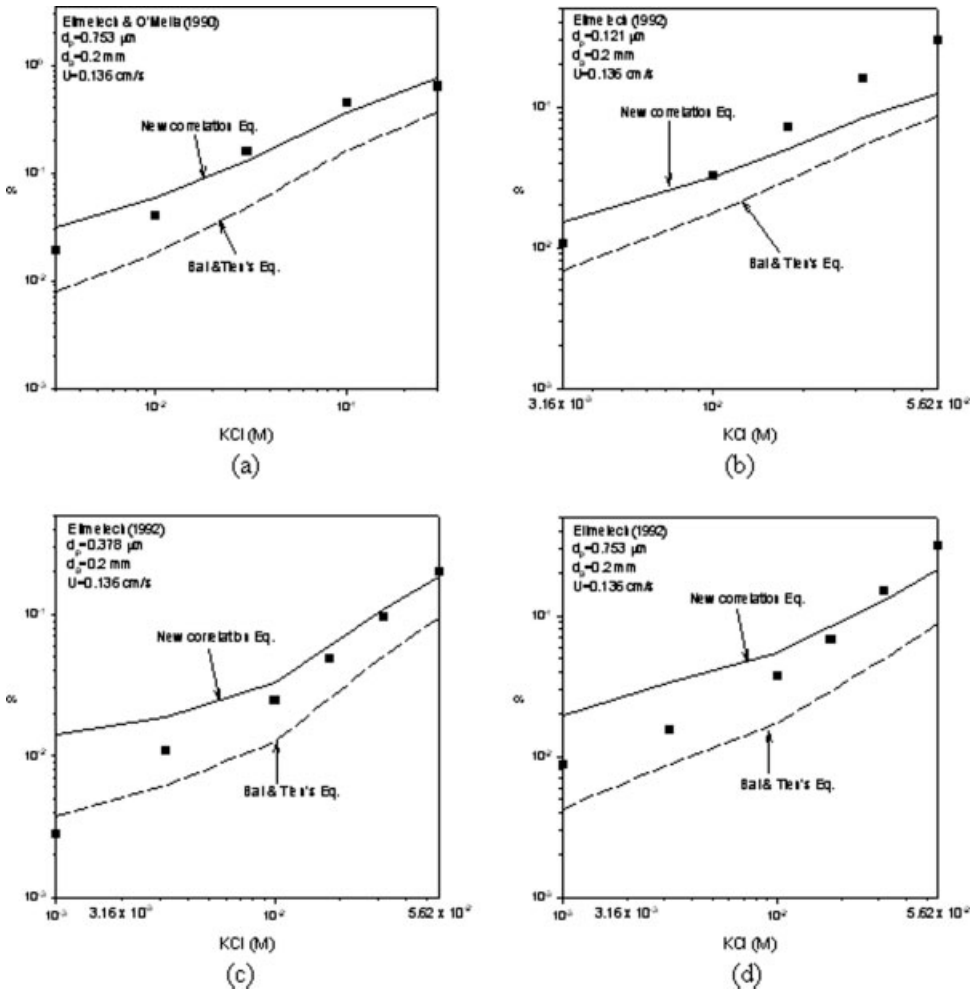

Figure 8. Comparison of experimental data of Elimelech[25] (Figure 8a) and Elimelech and O'Melia[24] (Figs. 8b–d) with predictions of filter coefficients (α) based on the Bai and Tien's equation of Eq. (13) (dashed lines) and the new correlation equation of Eq. (14) (solid lines).

With U = 0.136 cm/s and d_g = 0.2 mm, Figure 8(a) represents the comparison results when d_P = 0.753 μm, Figure 8(b) represents the comparison results when d_P = 0.121 μm, Figure 8(c) represents the comparison results when d_P = 0.378 μm and Figure 8(d) represents the comparison results when d_P = 0.753 μm.

where L is the length of the filter bed, C_{in} is the influent number concentration of colloidal particles, and C_{eff} is the effluent number concentration of the colloidal particles. By assuming the η_0 obtained at high ionic strength ($\geq$0.2 M) is equal to η_{0S}, then the experimental value of α defined in Eq. 1 corresponding to the different ionic strengths can be determined. The experimental values of α obtained by using Eq. 17 corresponding to different ionic strengths are also listed in the last column of Table 3. As shown in Figures 8 and 9, a common feature of those experimental determined α values is that their magnitudes decrease with the decrease of the ionic strength of the suspension. This is caused by an increase in the range of electrostatic double layer repulsion force and the height of the primary maximum energy barrier as the electrolyte concentration decreases. Also, as shown in these two figures, the present correlation equation always gives higher α values than those of Bai and Tien's equation when the electrolyte concentration is fixed. More importantly, better than that of Bai and Tien's equation, the present correlation equation can fit well with the experimental data especially for those sub-micro particles whose Brownian motion behavior can't be ignored. On the contrary, the present correlation equation shows less precision than the Bai and Tien's equation for larger particles, especially when the diameter of particles is as large as 11.4 μm adopted in the experiments of Vaidyanathan and Tien[26] (see Figure 9i). The comparison of the accuracy between the Bai and Tien's equation (Eq. 15) and the present new correlation equation (Eq. 16) is illustrated in Figure 10, which shows that the deviation of the data from the diagonal line is smaller for the present new correlation equation. Hence, the predictions of α based on the present new correlation equation yields better agreement with all those experimental data of Table 3 than that based on the Bai and Tien's equation.

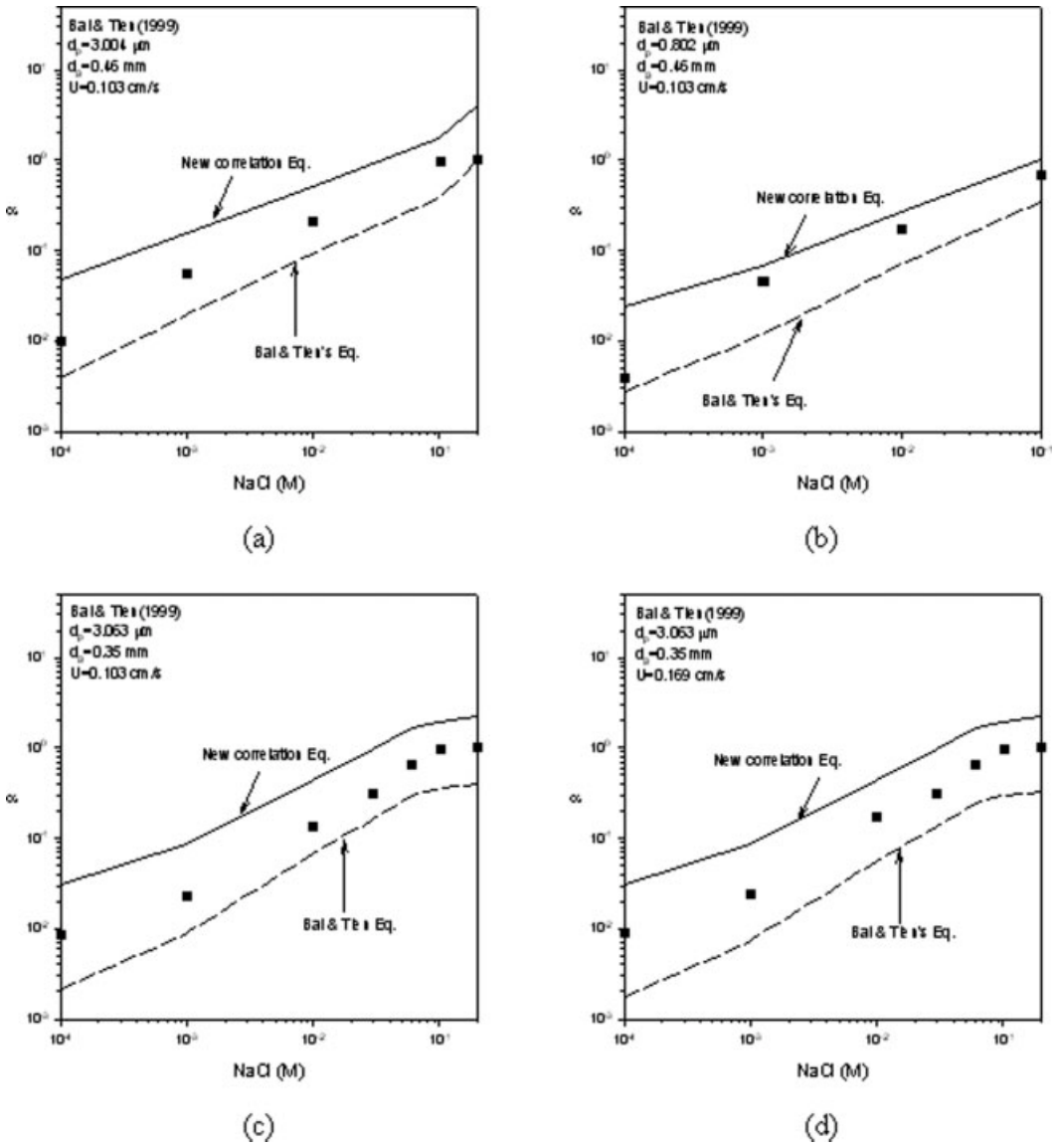

Figure 9. Comparison of experimental data of Bai and Tien[3] (Figures 9(a–f), Elimelech[25] (Figures 9g, h) and Vaidyanathan and Tien[26] (Figure 9i) with predictions of filter coefficients (α) based on the Bai and Tien's equation of Eq. (15) (dashed lines) and the new correlation equation of Eq. (16) (solid lines).

Conditions for eight figures are: (a) d_P = 3.004 μm, d_g = 0.46 mm, and U = 0.103 cm/s; (b) d_P = 0.802 μm, d_g = 0.46 mm and U = 0.103 cm/s; (c) d_P = 3.063 μm, d_g = 0.35 mm, and U = 0.103 cm/s; (d) d_P = 3.063 μ, d_g = 0.35 mm, and U = 0.169 cm/s; (e) d_P = 3.063 μm, d_g = 0.35 mm, and U = 0.272 cm/s; (f) d_P = 3.063 μm, d_g = 0.35 mm, and U = 0.103 cm/s; (g) d_P = 0.378 μm, d_g = 0.2 mm and U = 0.136 cm/s; (h) d_P = 0.753 μm, d_g = 0.2 mm, and U = 0.136 cm/s; (i) d_P = 11.4 μm, d_g = 0.345 mm, and U = 0.2 cm/s.

Conclusions

By adopting the triangular network model of using the Brownian dynamics simulation method, a new correlation equation on predicting the filter coefficient α under the unfavorable deposition conditions is successfully obtained based on the simulation results of calculating α values at different colloidal particle sizes filtrated in the filter bed. Taking the contributions of four deposition mechanisms, e.g., the Brownian diffusion, the DLVO interactions, the gravitational force and the interception into consideration, the present correlation equation shows remarkable agreement with those available experimental data especially for those submicro particles at different ionic strengths. The new correlation equation overcomes the shortage of previous correlations, which are unable to predict the filter coefficients under the

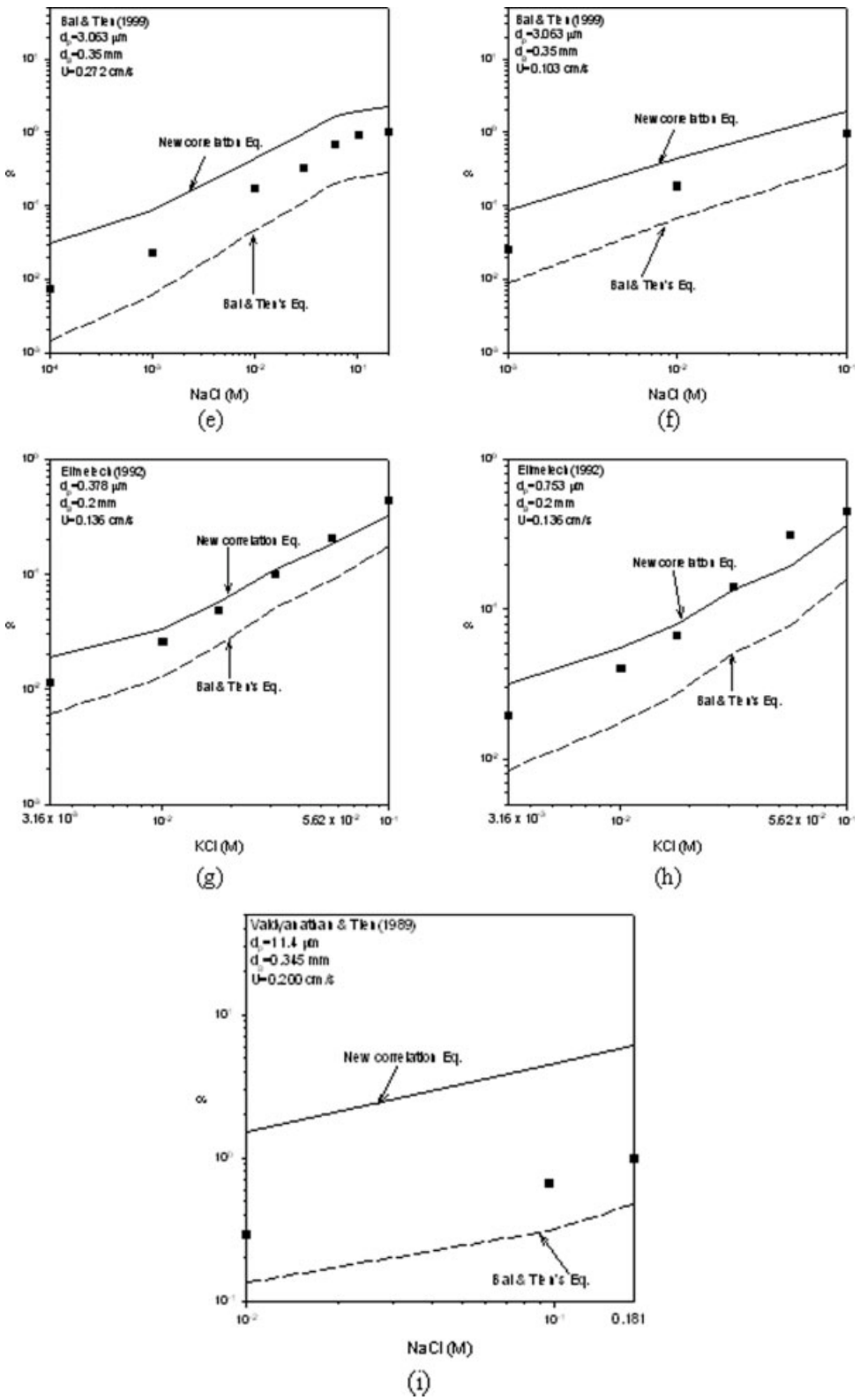

Figure 9. Continued

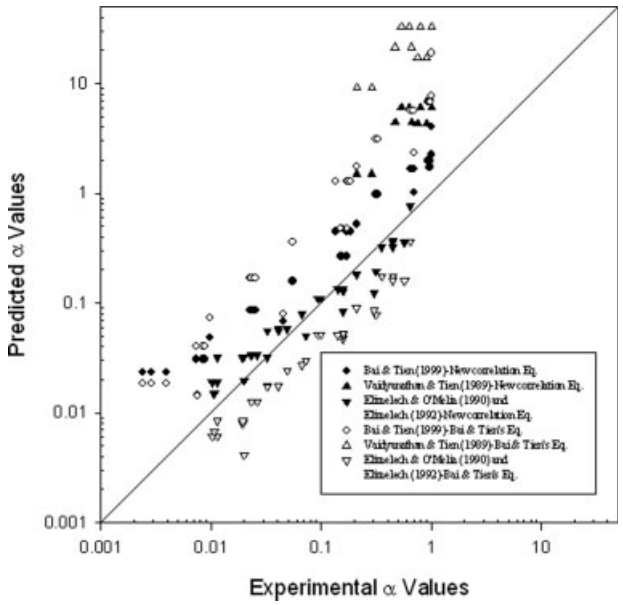

Figure 10. Comparison of experimental data shown in Table 3 with the new correlation equation of Eq. 16.

unfavorable deposition conditions where the ionic strengths are low.

Acknowledgments

The authors would like to express their sincere thanks to Prof. Chi Tien at Chemical Engineering Department of Syracuse University for his valuable suggestions on this work. The financial support received from the National Science Council of the Republic of China, research grant no. NSC-94-2214-E-029-003, is greatly appreciated.

Notation

A = Hamaker constant (Joule)
$A(t)$ = Gaussian white noise process in stochastic terms
A_{DLVO} = dimensionless group defined in Eq. 6
A_s = porosity-dependent parameter
a_i = random number shown in Eq. 3
a_p = particle radius μm
B, C = polynomial coefficients defined in Eq. 7 to represent the tangential component of the undisturbed flow field
C_{in} = inlet particle concentration (number of particles/cm^3)
C_{eff} = outlet particle concentration (number of particles/cm^3)
C_s = 1.16 for hydrosols; Cunningham correction factor
D_∞ = bulk diffusion coefficient of particles (cm^2/s)
d_c = constriction diameter of a constricted tube (μm)
d_g = spherical filter-grain diameter (μm)
d_{max} = maximum diameter of constricted tube (μm)
d_p = particle diameter (μm)
F_1, F_2, F_3 = retardation factors of normal vector, drag force, and shear vector respectively
F_{DL} = dimensionless electrostatic repulsion force
F_{Lo} = dimensionless van der Waals force
f_r^m, f_r^t = hydrodynamic retardation factor due to main flow and particle translation, respectively.
g = gravitational acceleration (cm/sec^2)
H = h_s/a_p; dimensionless separation distance
h = length of constricted tube (μm)
h_s = the smallest separation distance between the particle and the collector surface (μm)
k_BT = 0.41 $\times$ 10^{-20} Volt Coulomb at 20°C; Boltzmann constant times absolute temperature
L = length of the filter bed (cm)
m_p = mass of the particle (g)
N_A = attraction number
N_{DL} = double-layer force parameter, defined as κa_{pi}
$N_{E1} = va_{pi}(\xi_p^2 + \xi_g^2)/4k_BT$; first electrokinetic parameter
$N_{E2} = 2\left(\frac{\xi_p}{\xi_g}\right)\Big/\left[1 + \left(\frac{\xi_p}{\xi_g}\right)^2\right]$; second electrokinetic parameter
N_G = gravitational number
N_L = total number of bonds (pores) in the triangular network model
$N_{Lo} = A/6k_BT$
N_{Pe} = Peclect number
$N_R = d_p/d_g$; aspect ratio
r = position vector in the constricted tube model
r_c = constriction radius (μm)
r_f = radius of the spherical granular collector (μm)
r_{max} = maximum radius of constriction tube (μm)
r_{mean} = mean radius of pores (μm)
r_w = wall radius (μm)
t = time (s); scaled time
U = inlet flow velocity (cm/s)
u = fluid velocity vector
V_T = total interaction energy of DLVO theory (k_BT)
v_p = particle velocity vector
z = axial distance (μm)

Greek letters

α = filter coefficeint
α' = angle between the main flow and the line of centers of the particles
β = friction coefficient per unit mass of particle
$\gamma = (1 - \varepsilon)^{1/3}$
$\Delta\rho$ = density difference between particle and fluid (cm^3/g)
ε = filter porosity
η_0 = initial collection efficiency
η_{0S} = initial collection in the absence of the electrostatic repulsive force
κ = reciprocal of the electric double layer thickness (cm^{-1})
μ = viscosity of fluid (cp)
v = 89 $\times$ 10^{-12} Coulombs/Volt/cm for water; dielectric constant
ρ_p = particle density (cm^3/g)
ρ_f = fluid density (cm^3/g)
ζ_2 = normal coordinate of the particle center
ϕ_{DL} = dimensionless van der Waals attractive energy
ϕ_{Lo} = dimensionless electrostatic repulsive energy
ξ_p, ξ_g = surface (zeta) potentials of particle and grain collector, respectively, (mv)

Subscripts

0 = initial value
D = diffusion mechanism
DLVO = DLVO theory
G = gravitational mechanism
I = interception mechanism
i = the ith particle
mean = mean value
r = normal direction
t = tangential direction
θ = tangential component of the fluid field

Literature Cited

1. Verwey EJW, Overbeek JThG. *Theory of the Stability of Lyophobic Colloids*. Amsterdam, Netherlands: Elsevier Publishers, 1948.
2. Tien C, Ramarao BV. *Granular Filtration of Aerosols and Hydrosols, 2nd Edition*. Oxford, Great British: Elsevier Publishers, 2007.

3. Bai R, Tien C. Particle deposition under unfavorable surface interactions. *J Colloid Interface Sci*. 1999;218:488–499.
4. Vaidyanathan R, Tien C. Hydrosol deposition in granular media under unfavorable surface conditions. *Chemical Eng Sci*. 1991;46: 967–983.
5. Chang YI, Chan HC. Effects of three different network models on the filter coefficient of Brownian particles. *Separation Purification Technol*. 2006;51:291–302.
6. Payatakes AC, Tien C, Turian RM. Trajectory calculation of particle deposition in deep bed filtration, Part I: Model formulation. *AIChE J*. 1974;20:889–900.
7. Prieve DC, Ruckenstein E. Effect of London forces upon the rate of deposition of Brownian particles. *AIChE J*. 1974;20:1178–1187.
8. Elimelech M. Particle deposition on ideal collectors from dilute flowing suspensions: mathematical formulation, numerical solution, and simulations. *Separation Technol*. 1994;4:186–212.
9. Chang YI, Chen SC, Chan HC, Lee E. Network simulation for deep bed filtration of Brownian particles. *Chem Eng Sci*. 2004;59:4467–4479.
10. Sharma MM, Yortsos YC. A network model for deep bed filtration processes. *AIChE J*. 1987;33:1644–1653.
11. IMSL Fortran Library version 5.0, IMSL Corp. Rochester Hills, Michigan, 2005.
12. Chang YI, Chen SC, Lee E. Prediction of Brownian particle deposition in porous media using the constricted tube model. *J Colloid Interface Sci*. 2003;266:48–59.
13. Fedkiw P, Newman J. Mass transfer at high Peclet number for creeping flow in a packed-bed reactor. *AIChE J*. 1977;23:255–263.
14. Chow JCF, Soda K. Laminar flow in tubes with constriction. *Phys Fluids*. 1972;15:1701–1706.
15. Chiang HW, Tien C. Dynamics of deep-bed filtration, Part I: Analysis of two limiting situations. *AIChE J*. 1985;31:1349–1359.
16. Ramarao BV, Tien C, Mohan S. Calculation of single fiber efficiencies for interception and impaction with superposed Brownian motion. *J Aerosol Sci*. 1994;25:295–313.
17. Chang YI, Whang JJ. Deposition of Brownian particles in the presence of energy barriers of DLVO theory: effect of the dimensionless groups. *Chem Eng Sci*. 1998;53:3923–3939.
18. Kanaoka C, Emi H, Tarthapanichakoon W. Convective diffusional deposition and collection efficiency of aerosol on a dust-loaded fiber. *AIChE J*. 1983;29:895–902.
19. Rajagopalan R, Kim JS. Adsorption of brwonian particles in the presence of potential barriers: effect of different modes of double-layer interaction. *J Colloid Interface Sci*. 1981;83:428–448.
20. Yao KM, Habinian MT, O'Melia CR. Water and waste water fitration: concepts and applications. *Environ Sci Res*. 1971;5:1105–1112.
21. Happel J, Brenner H. 1st paperback Edition. *Low Reynolds Number Hydrodynamics*. The Hague, Netherlands: Martinus Nijhoff Publishers, 1983. see Chapter 7.
22. Rajagopalan R, Tien C. Trajectory analysis of deep bed filtration with the sphere-in-cell porous media model. *AIChE J*. 1976;22:523–533.
23. Tufenkji N, Elimelech M. Correlation equation for predicting single-collector efficiency in physicochemical filtration in saturated porous media. *Enviro Sci Technol*. 2004;38:529–536.
24. Elimelech M, O'Melia CR. Effect of particle size on collision efficiency in the deposition of Brownian particles with electrostatic energy barriers. *Langmuir*. 1990;6:1153–1163.
25. Elimelech M. Predicting collision efficiencies of colloidal particles in porous media. *Water Res*. 1992;26:1–8.
26. Vaidyanathan R, Tien C. Hydrosol deposition in granular beds—An experimental study. *Chem Eng Commun*. 1989;81:123–144.
27. SPSS version 13, SPSS Inc. Chicago, IL, 2005.

Manuscript received Oct. 2, 2007, and revision received Jan. 17, 2008.